This is a repository copy of *Mollow triplet for cavity-mediated laser cooling.*.

Mollow triplet for cavity-mediated laser cooling

Oleg Kim and Almut Beige

The School of Physics and Astronomy, University of Leeds, Leeds LS2 9JT, United Kingdom

(Dated: October 28, 2013)

Here we analyse cavity-mediated laser cooling for an experimental setup with an external trap which strongly confines the motion of a particle in the direction of the cavity axis. It is shown that the stationary state phonon number exhibits three sharp minima as a function of the atom-cavity detuning due to a direct atom-phonon-photon coupling term in the system Hamiltonian. These resonances have the same origin as the Mollow triplet in the resonance fluorescence of a laser-driven atomic system. It is shown that a laser-Rabi frequency-dependent atom-cavity detuning yields the lowest stationary state phonon number for a wide range of experimental parameters.

I.   INTRODUCTION

Laser sideband cooling allows to cool single, strongly-confined atomic particles to very low temperatures [1]. Its discovery opened the way for experiments which test the foundations of quantum physics and have applications ranging from quantum metrology to quantum computing [2]. Unfortunately, laser sideband cooling cannot be used to cool large numbers of trapped particles to very low temperatures. Moreover, laser sideband cooling cannot be used to cool particles with a very complex level structure, like molecules, very efficiently [3]. Alternative cooling techniques therefore receive a lot of attention in the literature. First indications that cavity-mediated laser cooling allows to cool trapped particles to low temperatures were found in Paris already in 1995 [4]. More systematic experimental studies of cavity-mediated laser cooling have subsequently been reported by several groups (cf. Refs. [5–13]).

The theory of cavity-mediated laser cooling of free particles was first discussed in Refs. [14, 15]. Later, Ritsch and collaborators [16, 17] and others [18–20] developed semiclassical theories to model cavity-mediated cooling processes. In 1993, Cirac *et al.* [21] introduced a master equation approach to analyse cavity-mediated laser cooling in detail. Since the precision of calculations which are based on master equations is easier to control than the precision of semiclassical calculations, this approach has been used by many authors to show a close analogy between laser-sideband and cavity-mediated laser cooling [22–27]. In this paper we use the same master equation approach as in Refs. [25, 26, 28] and analyse the cooling dynamics of the experimental setup in Fig. 1 with the help of linear differential equations, so-called rate equations, for expectation values.

In the following, we assume that an external trap confines the motion of a single particle in the direction of the cavity axis. This case is a special case of the general scenario considered in Refs. [24, 27]. As illustrated in Fig. 1, the particle should be placed in a node of the quantised standing wave cavity field mode. One way to achieve this is to drive the cavity and to create a strong optical lattice trapping potential. To initiate the cooling
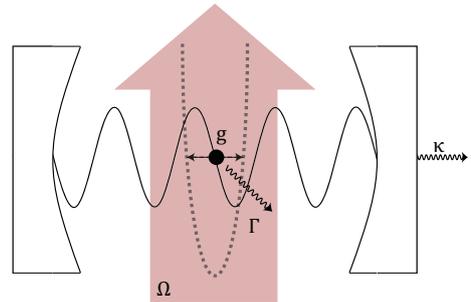
FIG. 1: (color online) Schematic view of the experimental setup. It consists of a resonantly driven atomic particle which is externally confined in the node of an optical cavity. Its motion is quantised in the direction of the cavity axis.

process, a laser field with Rabi frequency Ω should drive the particle from the side.

In cavity-mediated laser cooling, the reduction in the mean phonon number of the trapped particle is due to the continuous conversion of phonons into cavity photons. These phonons are permanently lost from the system when cavity photons leak out of the resonator. The result is a reduction of the kinetic energy of the trapped particle, ie. cooling. One of the roles of the atomic particle in the cooling process is to facilitate the phonon-photon conversion which needs to be accompanied by certain electronic transitions. The purpose of the applied laser field is to populate the atomic states which are involved in this process. Calculations which go beyond the scope of this paper have already shown that resonant laser driving of the atomic 0–1 transition supports the cooling process best. We therefore assume in the following zero laser detuning.

As we shall see below, the stationary state phonon number m_{ss} of the experimental setup in Fig. 1 exhibits three sharp minima as a function of the atom-cavity detuning δ. The corresponding atom-cavity resonances have the same origin as the Mollow triplet in the resonance fluorescence of a laser-driven atomic system [29, 30]. For relatively small spontaneous decay rates,

they are simply given by

$$\delta_0 \equiv \nu \quad \text{and} \quad \delta_\pm \equiv \nu \pm \Omega. \tag{1}$$

Although the experimental setup which we consider here has already been discussed in the literature [24, 27], the cooling potential of all three resonances has not yet been analysed in the literature. For a relatively wide range of experimental parameters, the previously unconsidered resonance $\delta = \delta_+$ yields a lower stationary state phonon number than the optimal detuning $\delta = \nu$ of laser side-band cooling [2]. Our calculations show that this cooling resonance is especially then of interest, when the spontaneous cavity decay rate κ is relatively large or when the phonon frequency ν is relatively small.

There are five sections in this paper. In Section II, we introduce the master equations for the description of the experimental setup shown in Fig. 1. We then use this equation to obtain a closed set of rate equations, ie. linear differential equations for the time evolution of expectation values. These can be used to model the time evolution of the mean phonon number m up to second order in the Lamb-Dicke parameter η. Before doing so, Section III uses a simple argument to identify the relevant cooling and heating resonances. A detailed analysis of the cooling process with analytical and numerical results can be found in Section IV. Finally, we summarise our findings in Section V.

II. THEORETICAL MODEL

Let us now have a closer look at the Hamiltonian of the experimental setup shown in Fig. 1. In the usual dipole and rotating wave approximation, it equals

$$\begin{aligned} H &= \hbar\omega_0\,\sigma^+\sigma^- + \hbar\nu\,b^\dagger b + \hbar\omega_{\text{cav}}\,c^\dagger c \\ &\quad + \hbar g\,\sin\left(\mathbf{k}_{\text{cav}}\cdot\mathbf{r}\right)c\sigma^+ + \text{H.c.} \\ &\quad + \frac{1}{2}\hbar\Omega\,\sigma^+\,e^{-i\omega_0 t} + \text{H.c.} \end{aligned} \tag{2}$$

Here $\hbar\omega_0$, $\hbar\nu$, and $\hbar\omega_{\text{cav}}$ denote the energy difference between the atomic ground state $|0\rangle$ and the excited state $|1\rangle$, the free energy of a single phonon, and the free energy of a cavity photon. Moreover, $\sigma^+ \equiv |1\rangle\langle 0|$ and $\sigma^- \equiv |0\rangle\langle 1|$, while b and c are phonon and photon annihilation operators with bosonic commutator relations,

$$[b, b^\dagger] = [c, c^\dagger] = 1. \tag{3}$$

The second line in Eq. (2) takes the atom-cavity interaction at the position $\mathbf{r}$ of the trapped particle into account. Here g is the atom-cavity coupling constant and $\mathbf{k}_{\text{cav}}$ is the wave vector of the cavity field. The third line describes the resonant driving of the particle with a laser with Rabi frequency Ω and frequency ω_0.

In this paper, we assume an external trap which confines the motion of the particle in the direction of the cavity axis. We denote the trap centre by $\mathbf{R}$ and the displacement of the atom from the trap center by $\mathbf{x}$ such that its position $\mathbf{r}$ is given by $\mathbf{r} = \mathbf{R} + \mathbf{x}$. Considering the center of mass motion of the trapped particle quantised with the phonon annihilation operator b from above yields

$$\mathbf{k}_{\text{cav}} \cdot \mathbf{x} = \eta(b + b^\dagger). \tag{4}$$

The Lamb-Dicke parameter η in this equation is a measure for the strength of the trapping potential. Usually, one has

$$\eta \ll 1. \tag{5}$$

For a wide range of particle positions $\mathbf{r}$, the atom-phonon-photon interaction is therefore only relatively weak. In order to maximise it, we assume in the following that $\mathbf{R}$ points at a node of the cavity field which implies $e^{-i\mathbf{k}_{\text{cav}}\cdot\mathbf{R}} = \pm 1$. Hence

$$\sin\left(\mathbf{k}_{\text{cav}}\cdot\mathbf{r}\right) = \pm\eta\left(b + b^\dagger\right) + \mathcal{O}(\eta^3). \tag{6}$$

Substituting this equation into Eq. (2) and going into the interaction picture with respect to

$$H_0 = \hbar\omega_0(\sigma^+\sigma^- + c^\dagger c), \tag{7}$$

we obtain the time-independent interaction Hamiltonian

$$\begin{aligned} H_{\text{I}} &= \hbar\nu\,b^\dagger b + \hbar\delta\,c^\dagger c + \frac{1}{2}\hbar\Omega\left(\sigma^- + \sigma^+\right) \\ &\quad + \hbar\eta g\left(b + b^\dagger\right)(\sigma^+ c + \sigma^- c^\dagger) + \mathcal{O}(\eta^3) \end{aligned} \tag{8}$$

in the usual Lamb-Dicke approximation. Here we ignored the minus sign in Eq. (6), since this phase factor has no real physical consequences [32].

The main difference between laser-sideband [1, 2] and cavity-mediated laser cooling is that, in the latter case, the atomic raising operator σ^+ in the cooling Hamiltonian is replaced by the cavity photon creation operator $c^\dagger$. Hence, the cooling efficiency depends strongly on the spontaneous cavity decay rate κ and not only on the spontaneous atom decay rate Γ. To model this, spontaneous photon emission is in the following taken into account by the quantum optical master equation

$$\begin{aligned} \dot{\rho}_{\text{I}} &= -\frac{i}{\hbar}\left[H_{\text{I}}, \rho_{\text{I}}\right] + \frac{1}{2}\kappa\left(2c\rho_{\text{I}}c^\dagger - c^\dagger c\rho_{\text{I}} - \rho_{\text{I}}c^\dagger c\right) \\ &\quad + \frac{1}{2}\Gamma\left(2\sigma^-\rho_{\text{I}}\sigma^+ - \sigma^+\sigma^-\rho_{\text{I}} - \rho_{\text{I}}\sigma^+\sigma^-\right). \end{aligned} \tag{9}$$

In the following, we use this equation to analyse the cooling process on a time scale proportional to η^2. But before doing so, let us have a closer look at the expected cooling and heating resonances.

III. EXPECTED COOLING AND HEATING RESONANCES

Phonons have no spontaneous decay rate. To initiate the cooling process, it is therefore important to convert

them into particles with a non-zero spontaneous decay rate, like cavity photons. One of the roles of the atomic particle is to facilitate this conversion. By changing its electronic state, the atomic particle supports the conversion of a phonon into a cavity photon. When the photon subsequently leaks out of the cavity, a phonon is permanently lost which implies cooling. In order to make the cooling process as efficient as possible, the detunings of the experimental setup in Fig. 1 should be adjusted such that cooling transitions become resonant. Moreover, all heating transitions should be as off-resonant as possible. For the experimental setup which we consider here, this means that at least some of the $bc^\dagger$-terms in the Hamiltonian need to be in resonance, while resonance of $b^\dagger c^\dagger$ terms should be avoided.

In order to identify the relevant cooling and heating resonances and to get more insight into the dynamics induced by the Hamiltonian H_I, we now change into a dressed state picture. To do so, we diagonalise the laser driving term, ie. the atomic operator $\sigma_x = \sigma^- + \sigma^+$, in Eq. (12). The eigenvalues and eigenvectors of σ_x are $\lambda_\pm = \pm 1$ and

$$|\lambda_\pm\rangle = \frac{1}{\sqrt{2}}\big(|0\rangle \pm |1\rangle\big),\qquad(10)$$

respectively. Using this notation, we find that

$$\sigma^\pm = \frac{1}{2}\big(|\lambda_+\rangle\langle\lambda_+| - |\lambda_-\rangle\langle\lambda_-| \pm |\lambda_+\rangle\langle\lambda_-| \mp |\lambda_-\rangle\langle\lambda_+|\big).\qquad(11)$$

Consequently, the Hamiltonian H_I in Eq. (8) can be written as

$$\begin{aligned} H_I =\ & \hbar\nu\, b^\dagger b + \hbar\delta\, c^\dagger c + \frac{1}{2}\hbar\Omega\left(|\lambda_+\rangle\langle\lambda_+| - |\lambda_-\rangle\langle\lambda_-|\right) \\ & + \frac{1}{2}\hbar\eta g\,(b+b^\dagger)(c+c^\dagger)\big(|\lambda_+\rangle\langle\lambda_+| - |\lambda_-\rangle\langle\lambda_-|\big), \\ & + \frac{1}{2}\hbar\eta g\,(b+b^\dagger)(c-c^\dagger)\big(|\lambda_+\rangle\langle\lambda_-| - \text{H.c.}\big). \end{aligned}\qquad(12)$$

To remove all the terms in the first line of this equation from H_I, we now go into a further interaction picture and obtain the interaction Hamiltonian $\tilde{H}_I$,

$$\begin{aligned} \tilde{H}_I =\ & \frac{1}{2}\hbar\eta g\left[e^{-i(\delta+\nu)t}\, bc + e^{-i(\delta-\nu)t}\, bc^\dagger + \text{H.c.}\right] \\ & \times\big(|\lambda_+\rangle\langle\lambda_+| - |\lambda_-\rangle\langle\lambda_-|\big) \\ & + \frac{1}{2}\hbar\eta g\left[e^{-i(\delta+\nu)t}\, bc - e^{-i(\delta-\nu)t}\, bc^\dagger - \text{H.c.}\right] \\ & \times\big(e^{i\Omega t}\,|\lambda_+\rangle\langle\lambda_-| - \text{H.c.}\big). \end{aligned}\qquad(13)$$

To assure that at least one of the $bc^\dagger$ terms in the above Hamiltonian becomes time-independent, the atom-cavity detuning δ needs to equal one of the three detunings δ_0 and $\delta_\pm$ in Eq. (1). These three resonances are the three cooling resonances of the cooling process which we consider here.

Moreover, all heating terms, ie. all $b^\dagger c^\dagger$ terms, should oscillate rapidly in time. This means, the atom-cavity detuning δ should stay away as far as possible from the three detunings

$$\mu_0 \equiv -\nu \quad\text{and}\quad \mu_\pm \equiv -\nu \pm \Omega\,.\qquad(14)$$

These are the three heating resonances of the cooling process. One can easily check that the distance between any neighboring cooling or heating resonances equals the laser Rabi frequency Ω, ie. $|\delta_0 - \delta_\pm|$ and $|\mu_0 - \mu_\pm|$. The same applies for the resonances of a laser-driven atomic two-level system inside a quantised field [29]. This means, the δ resonances in Eq. (1) and the μ resonances in Eq. (14), respectively, form a so-called Mollow triplet.

IV. DETAILED ANALYSIS OF THE COOLING PROCESS

The discussion in the previous section tells us for which atom-cavity detunings we can expect relatively efficient cooling of the trapped particle, as long as the spontaneous decay rates κ and Γ remain relatively small. To learn more about the cooling process and to study the effect of relatively large spontaneous decay rates, we now analyse the above described cooling process in more detail. To do so, we introduce a closed set of rate equations. These are linear differential equations for the time evolution of expectation values. Using the master equation (9), one can show that the time evolution of the expectation value of an arbitrary operator A_I in the interaction picture is given by

$$\begin{aligned} \langle\dot{A}_I\rangle =\ & -\frac{i}{\hbar}\langle[A_I, H_I]\rangle + \frac{1}{2}\kappa\left\langle 2c^\dagger A_I c - A_I c^\dagger c - c^\dagger c A_I\right\rangle \\ & + \frac{1}{2}\Gamma\left\langle 2\sigma^+ A_I \sigma^- - A_I \sigma^+\sigma^- - \sigma^+\sigma^- A_I\right\rangle. \end{aligned}\qquad(15)$$

Here we are especially interested in the time evolution of the mean phonon number

$$m \equiv \langle b^\dagger b\rangle\,.\qquad(16)$$

Additional expectation values are taken into account in order to obtain a closed set of rate equations which accurately describe the experimental setup in Fig. 1 on a time scale proportional to η^2.

In the following, we assume that the atom-phonon-photon interaction constant ηg is either much smaller than the atom-cavity detuning δ, or much smaller than the cavity decay rate κ, or much smaller than the phonon frequency ν,

$$\eta g \ll \delta,\,\kappa,\,\text{or}\,\nu\,.\qquad(17)$$

As we shall see below, this condition guarantees that the mean phonon number m evolves on a much slower time scale than all other expectation values which are involved in the cooling process. It guarantees that the time evolution of m is much slower than the inner dynamics of the

atom-cavity-phonon system. No conditions, other than Eq. (17), need to be imposed for the following calculations to apply.

A. The relevant expectation values

As we shall see below, in order to obtain a closed set of cooling equations, including one for the time evolution of the mean phonon number m up to order η^2, we need to consider the expectation values of certain mixed operators X_{ijk} of the form

$$X_{ijk} \equiv B_i \Sigma_j C_k \qquad (18)$$

with the B, Σ, and C operators defined such that

$$
\begin{aligned}
(B_0, \Sigma_0, C_0) &\equiv (1, 1, 1) \,, \\
(B_1, \Sigma_1, C_1) &\equiv (b^\dagger b, \sigma^+ \sigma^-, c^\dagger c) \,, \\
(B_2, \Sigma_2, C_2) &\equiv (b + b^\dagger, \sigma^- + \sigma^+, c + c^\dagger) \,, \\
(B_3, \Sigma_3, C_3) &\equiv \mathrm{i}(b - b^\dagger, \sigma^- - \sigma^+, c - c^\dagger) \,, \\
(B_4, C_4) &\equiv (b^2 + b^{\dagger 2}, c^2 + c^{\dagger 2}) \,, \\
(B_5, C_5) &\equiv \mathrm{i}(b^2 - b^{\dagger 2}, c^2 - c^{\dagger 2}) \,.
\end{aligned} \qquad (19)
$$

Using these operators, the Hamiltonian H_{I} in Eq. (8) becomes

$$
\begin{aligned}
H_{\mathrm{I}} = {}& \hbar \nu \, B_1 + \hbar \delta \, C_1 + \frac{1}{2} \hbar \Omega \, \Sigma_2 \\
& + \frac{1}{2} \hbar \eta g \, B_2 (\Sigma_2 C_2 + \Sigma_3 C_3) \,.
\end{aligned} \qquad (20)
$$

In the following, we use this representation of the Hamiltonian, since the X operators obey relatively simple commutator relations.

Moreover, we denote their expectation values by

$$x_{ijk} \equiv \langle X_{ijk} \rangle \,. \qquad (21)$$

Since all the operators X_{ijk} are Hermitian, the variables x_{ijk} are all real. To distinguish terms in different orders in η more easily, we adopt the notation

$$x_{ijk} \equiv x_{ijk}^{(0)} + x_{ijk}^{(1)} + \dots \qquad (22)$$

throughout the remainder of this manuscript, while the mean phonon number m is written as

$$m \equiv m^{(0)} + m^{(1)} + \dots \qquad (23)$$

and so on. The superscripts indicate the scaling of the contribution of the respective variable in η.

B. Time evolution in zeroth order in η

First we have a look at the $\eta = 0$ case. This means, we assume that there is no coupling between phonon,

photon, and atomic states. Hence the cavity remains in its vacuum state and

$$\langle C_k \rangle^{(0)} \equiv 0 \qquad (24)$$

for $k = 1, \dots, 5$. Analogously, or by using Eqs. (15) and (20), one can show that

$$\dot{m}^{(0)} = 0 \,. \qquad (25)$$

This tells us that there is no cooling in zeroth order in η. Moreover we find that

$$
\begin{aligned}
\langle \dot{B}_2 \rangle^{(0)} &= -\nu \langle B_3 \rangle^{(0)} \,, \quad \langle \dot{B}_3 \rangle^{(0)} = \nu \langle B_2 \rangle^{(0)} \,, \\
\langle \dot{B}_4 \rangle^{(0)} &= -2\nu \langle B_5 \rangle^{(0)} \,, \quad \langle \dot{B}_5 \rangle^{(0)} = 2\nu \langle B_4 \rangle^{(0)} \,.
\end{aligned} \qquad (26)
$$

When solving these rate equations, we find that the phonon coherences $\langle B_2 \rangle^{(0)}$ to $\langle B_5 \rangle^{(0)}$ oscillate around zero on time scales given by the phonon frequency ν. When analysing the cavity-mediated cooling process on a much longer time scale, the above phonon coherences can be adiabatically eliminated from the system dynamics. Setting their time derivatives in Eq. (26) equal to zero yields

$$\langle B_i \rangle^{(0)} \equiv 0 \qquad (27)$$

with $i = 2, \dots, 5$. Notice that we only use this equation to analyse the cooling dynamics of our system. In this case, Eq. (27) is well justified, since the effective cooling rate γ_{c} of the experimental setup which we consider here (see below) scales as η^2.

After introducing the short hand notation $z_j \equiv \langle \Sigma_j \rangle^{(0)}$ for expectation values of the electronic states of the trapped particle, one can show that

$$
\dot{z}_1 = \frac{1}{2} \Omega \, z_3 - \Gamma z_1 \,, \quad \dot{z}_2 = -\frac{1}{2} \Gamma z_2 \,,
$$
$$
\dot{z}_3 = \Omega (1 - 2z_1) - \frac{1}{2} \Gamma z_3 \qquad (28)
$$

in zeroth order in η. These expectation values reach a stationary state relatively quickly. When analysing processes on the time scale given by the cooling rate γ_{c}, these too can be adiabatically eliminated and approximated by their stationary state solutions. Doing so, we find that

$$(z_1, z_2, z_3) = \left(\frac{\Omega^2}{\Gamma^2 + 2\Omega^2}, 0, \frac{2\Gamma\Omega}{\Gamma^2 + 2\Omega^2} \right) \,. \qquad (29)$$

Before using these results to derive an effective cooling equation for the mean phonon number m, we notice that

$$x_{ijk}^{(0)} = \langle B_i \rangle^{(0)} \langle \Sigma_j \rangle^{(0)} \langle C_k \rangle^{(0)} \qquad (30)$$

when $\eta = 0$, since all three subsystems evolve independently in this case.

C. Time evolution in first order in η

Let us now have a closer look at the differential equations which describe the time evolution of m and the x_{ijk}'s in first order in η. Using Eqs. (15) and (20) we find for example that

$$\dot{m}^{(1)} = \frac{1}{2}\eta g \left(x_{322}^{(0)} + x_{333}^{(0)} \right).\qquad(31)$$

Unfortunately, Eq. (30) implies $x_{322}^{(0)} = x_{333}^{(0)} = 0$ which yields

$$\dot{m}^{(1)} = 0.\qquad(32)$$

As in other laser cooling schemes of atomic particles, the mean phonon number m changes only on the very slow time scale given by η^2. As we shall see below, we obtain a non-zero time derivative of m, when we calculate x_{322} and x_{333} up to first order in η. Therefore, we now have a closer look at these expectation values.

Taking the results in Eqs. (24), (27), (29), and (30) into account, one can show that

$$\dot{x}_{202}^{(1)} = -\nu\, x_{302}^{(1)} - \delta\, x_{203}^{(1)} - \eta g \left(1 + 2m^{(0)} \right) z_3 - \frac{1}{2}\gamma_0\, x_{202}^{(1)},$$

$$\dot{x}_{203}^{(1)} = -\nu\, x_{303}^{(1)} + \delta\, x_{202}^{(1)} + \eta g \left(1 + 2m^{(0)} \right) z_2 - \frac{1}{2}\gamma_0\, x_{203}^{(1)}$$

$$\dot{x}_{302}^{(1)} = \nu\, x_{202}^{(1)} - \delta\, x_{303}^{(1)} + \eta g\, z_2 - \frac{1}{2}\gamma_0\, x_{302}^{(1)}$$

$$\dot{x}_{303}^{(1)} = \nu\, x_{203}^{(1)} + \delta\, x_{302}^{(1)} + \eta g\, z_3 - \frac{1}{2}\gamma_0\, x_{303}^{(1)},\qquad(33)$$

and

$$\dot{x}_{212}^{(1)} = -\nu\, x_{312}^{(1)} - \delta\, x_{213}^{(1)} + \frac{1}{2}\Omega\, x_{232}^{(1)} - \frac{1}{2}\gamma_2\, x_{212}^{(1)},$$

$$\dot{x}_{213}^{(1)} = -\nu\, x_{313}^{(1)} + \delta\, x_{212}^{(1)} + \frac{1}{2}\Omega\, x_{233}^{(1)} - \frac{1}{2}\gamma_2\, x_{213}^{(1)},$$

$$\dot{x}_{312} = \nu\, x_{212}^{(1)} - \delta\, x_{313}^{(1)} + \frac{1}{2}\Omega\, x_{332}^{(1)} - \frac{1}{2}\gamma_2\, x_{312}^{(1)},$$

$$\dot{x}_{313}^{(1)} = \nu\, x_{213}^{(1)} + \delta\, x_{312}^{(1)} + \frac{1}{2}\Omega\, x_{333}^{(1)} - \frac{1}{2}\gamma_2\, x_{313}^{(1)}.\qquad(34)$$

Moreover, one can show that

$$\dot{x}_{222}^{(1)} = -\nu\, x_{322}^{(1)} - \delta\, x_{223}^{(1)} - \frac{1}{2}\gamma_1\, x_{222}^{(1)},$$

$$\dot{x}_{223}^{(1)} = -\nu\, x_{323}^{(1)} + \delta\, x_{222}^{(1)} + 2\eta g \left(1 + 2m^{(0)} \right) z_1 - \frac{1}{2}\gamma_1\, x_{223}^{(1)},$$

$$\dot{x}_{322}^{(1)} = \nu\, x_{222}^{(1)} - \delta\, x_{323}^{(1)} + 2\eta g\, z_1 - \frac{1}{2}\gamma_1\, x_{322}^{(1)},$$

$$\dot{x}_{323}^{(1)} = \nu\, x_{223}^{(1)} + \delta\, x_{322}^{(1)} - \frac{1}{2}\gamma_1\, x_{323}^{(1)},\qquad(35)$$

and

$$\dot{x}_{232}^{(1)} = -\nu\, x_{332}^{(1)} - \delta\, x_{233}^{(1)} + \Omega \left(x_{202}^{(1)} - 2x_{212}^{(1)} \right)$$
$$\qquad -2\eta g \left(1 + 2m^{(0)} \right) z_1 - \frac{1}{2}\gamma_1\, x_{232}^{(1)},$$

$$\dot{x}_{233}^{(1)} = -\nu\, x_{333}^{(1)} + \delta\, x_{232}^{(1)} + \Omega \left(x_{203}^{(1)} - 2x_{213}^{(1)} \right) - \frac{1}{2}\gamma_1\, x_{233}^{(1)},$$

$$\dot{x}_{332}^{(1)} = \nu\, x_{232}^{(1)} - \delta\, x_{333}^{(1)} + \Omega \left(x_{302}^{(1)} - 2x_{312}^{(1)} \right) - \frac{1}{2}\gamma_1\, x_{332}^{(1)},$$

$$\dot{x}_{333}^{(1)} = \nu\, x_{233}^{(1)} + \delta\, x_{332}^{(1)} + \Omega \left(x_{303}^{(1)} - 2x_{313}^{(1)} \right) + 2\eta g\, z_1$$
$$\qquad -\frac{1}{2}\gamma_1\, x_{333}^{(1)}.\qquad(36)$$

Here the effective spontaneous decay rates γ_n are defined such that

$$\gamma_n \equiv \kappa + n\,\Gamma.\qquad(37)$$

As we shall see below (cf. Eq. (39)), these equations indeed constitute a closed set of rate equations when combined with the differential equation for the time evolution of the mean phonon number m in second order in η.

D. An effective cooling equation

The previous two subsections have shown that there is no time evolution of the mean phonon number m in zeroth and first order in η (cf. Eqs. (25) and (32)). Going an order higher in η and using again Eqs. (15) and (20) yields

$$\dot{m}^{(2)} = \frac{1}{2}\eta g \left(x_{322}^{(1)} + x_{333}^{(1)} \right).\qquad(38)$$

To calculate the x-coherences in this equation, we employ condition (17). This condition allows us to calculate the coherences $x_{ijk}^{(1)}$ in Eqs. (33)–(36) via an adiabatic elimination. Doing so and setting for example the time derivatives of the coherences $x_{ijk}^{(1)}$ with $j = 2$ in Eq. (35) equal to zero, we obtain an expression for $x_{322}^{(1)}$. To calculate $x_{333}^{(1)}$, the remaining 12 rate equations have to be taken into account. Setting them equal to zero and substituting the resulting expressions for $x_{322}^{(1)}$ and $x_{333}^{(1)}$ into Eq. (38), we finally find that

$$\dot{m}^{(2)} = \frac{2\eta^2 g^2 \Omega^2}{\Gamma^2 + 2\Omega^2} \left\{ \frac{\gamma_1}{\gamma_1^2 + \xi_+^2} + \frac{\left(\gamma_0 \gamma_1 \gamma_2 + \gamma_{-1} \xi_+^2\right)\left(\gamma_2^2 + \xi_+^2\right) + 4\Omega^2 \left(\gamma_0 \gamma_2^2 + \gamma_4 \xi_+^2\right)}{\left(\gamma_0^2 + \xi_+^2\right)\left[\left(\gamma_1^2 + \xi_+^2\right)\left(\gamma_2^2 + \xi_+^2\right) + 8\Omega^2 \left(\gamma_1 \gamma_2 - \xi_+^2\right) + 16\Omega^4\right]} \right\} \left(1 + m^{(0)}\right)$$

$$-\frac{2\eta^2 g^2 \Omega^2}{\Gamma^2 + 2\Omega^2} \left\{ \frac{\gamma_1}{\gamma_1^2 + \xi_-^2} + \frac{\left(\gamma_0 \gamma_1 \gamma_2 + \gamma_{-1} \xi_-^2\right)\left(\gamma_2^2 + \xi_-^2\right) + 4\Omega^2 \left(\gamma_0 \gamma_2^2 + \gamma_4 \xi_-^2\right)}{\left(\gamma_0^2 + \xi_-^2\right)\left[\left(\gamma_1^2 + \xi_-^2\right)\left(\gamma_2^2 + \xi_-^2\right) + 8\Omega^2 \left(\gamma_1 \gamma_2 - \xi_-^2\right) + 16\Omega^4\right]} \right\} m^{(0)} \qquad (39)$$

with the parameter $\xi_\pm$ defined as

$$\xi_\pm \equiv 2(\delta \pm \nu) \qquad (40)$$

and with the γ_n defined as in Eq. (37).

Setting the time derivative $\dot{m}^{(2)}$ in Eq. (39) equal to zero yields an analytical expression for the stationary state phonon number m_{ss} of the proposed cooling process in zeroth order in η. Unfortunately, this expression is relatively complex and looking at it does not yield much insight into the considered cavity-mediated laser cooling process. In the following, we therefore only notice that the time evolution of the mean phonon number m is to a very good approximation given by a differential equations of the form

$$\dot{m} = -\gamma_c m + c, \qquad (41)$$

where γ_c is an effective cooling rate and where c is a constant. Taking Eqs. (25) and (32) into account and comparing Eq. (41) with Eq. (39) confirms that both γ_c and c scale as η^2. The comparison also yields analytical expressions for $\gamma_c^{(2)}$ and $c^{(2)}$. In the following, we discuss the dependence of $\gamma_c^{(2)}$ and of the stationary state phonon number $m_{ss}^{(0)}$,

$$m_{ss}^{(0)} = c^{(2)}/\gamma_c^{(2)}, \qquad (42)$$

on the different experimental parameters of the atom-cavity system in Fig. 1.

E. Confirmation of the expected cooling and heating resonances

Before doing so, let us have a closer look at Eq. (39). Suppose that the laser driving is so weak that all the Ω^2 terms in Eq. (39) become negligible. In this case, we find that

$$m_{ss}^{(0)} = \frac{\kappa^2 + 4(\delta - \nu)^2}{16\delta\nu}. \qquad (43)$$

This stationary state phonon number is exactly the same as m_{ss} for laser sideband cooling of a trapped particle in free space [1, 2, 28] but with Γ replaced by κ. For relatively small cavity decay rates κ, it assumes its minimum when $\delta = \delta_0$ with δ_0 defined as in Eq. (1). Looking only at the case of weak laser driving, one might

indeed conclude that there is only a single cooling resonance and a very close analogy between laser sideband and cavity-mediated laser cooling. Instead, this paper illustrates that atom-cavity-phonon systems can exhibit a much richer inner dynamics than systems with only atom-phonon interactions.

Another interesting parameter regime is the one where $\Omega, \xi_\pm \gg \kappa, \Gamma$. In this case, Eq. (39) simplifies to

$$\dot{m}^{(2)} = \eta^2 g^2 \left\{ \frac{\gamma_1}{\xi_+^2} + \frac{\gamma_{-1} \xi_+^2 + 4\gamma_4 \Omega^2}{\xi_+^4 - 8\Omega^2 \xi_+^2 + 16\Omega^4} \right\} \left(1 + m^{(0)}\right)$$

$$-\eta^2 g^2 \left\{ \frac{\gamma_1}{\xi_-^2} + \frac{\gamma_{-1} \xi_-^2 + 4\gamma_4 \Omega^2}{\xi_-^4 - 8\Omega^2 \xi_-^2 + 16\Omega^4} \right\} m^{(0)}. \quad (44)$$

The corresponding stationary state phonon number $m_{ss}^{(0)}$ equals zero when $\xi_-^2 = 4\Omega^2$, ie. when δ equals either δ_- or δ_+ in Eq. (1). This simple analysis confirms the presence of the two additional laser-Rabi frequency dependent cooling resonances $\delta_\pm$. However, notice that the above constraint $\xi_- \gg \kappa, \Gamma$ excludes the case where $\delta = \nu$. Hence this simple calculation returns only two of the three cooling resonances.

We now return to Eq. (39) and use it to calculate the stationary state phonon number $m_{ss}^{(0)}$ for the experimental setup in Fig. 1 for concrete experimental parameters. Fig. 2 shows $m_{ss}^{(0)}$ as a function of the atom-cavity detuning δ for a relatively wide range of parameters. To illustrate that the predictions in Section III apply, even for relatively large spontaneous decay rates, we choose κ and Γ to be of about the same order of magnitude as the phonon frequency ν and the atom-cavity detuning δ. For relatively large laser Rabi frequencies Ω, we indeed observe three distinct cooling resonances with sharp local minima of the stationary state phonon number m_{ss}. These are the atom-cavity detunings δ_0 and $\delta_\pm$ which we defined in Eq. (1). In contrast to this and in good agreement with the discussion in Section III, the stationary state phonon number $m_{ss}^{(0)}$ increases significantly, when δ approaches one of the three heating resonances μ_0 and $\mu_\pm$ in Eq. (14). Only, when Ω becomes much smaller than ν, then the cooling resonances and the heating resonances, respectively, become all the same. In this case, cooling occurs only for $\delta = \nu$ and extreme heating occurs for $\delta = -\nu$.
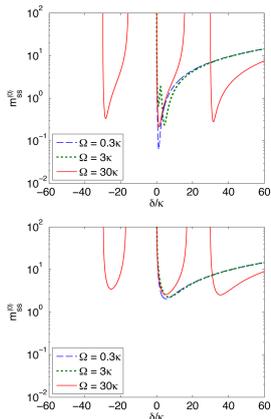
FIG. 2: (color online) Logarithmic plot of the stationary state phonon number $m_{\rm ss}^{(0)}$ as a function of the atom-cavity detuning δ for three different Rabi frequencies Ω and $\nu = \Gamma$, while $\kappa = \Gamma$ (upper figure) and $\kappa = 10\,\Gamma$ (lower figure). This figure has been obtained from Eq. (39) by setting $\dot{m}^{(2)}$ equal to zero and clearly illustrates the presence of the cooling and heating resonances which we identified in Eqs. (1) and (14).

F. A comparison of the three cooling resonances

To find out how to best cool a trapped particle when using the experimental setup in Fig. 1, we now compare the stationary state phonon numbers $m_{\rm ss}^{(0)}$ and the effective cooling rates $\gamma_{\rm c}^{(2)}$ of the three cooling resonances δ_0 and $\delta_\pm$ with each other. When comparing the expressions for $\dot{m}^{(2)}$ in Eqs. (39) and (41), we find that $\gamma_{\rm c}^{(2)}$ becomes independent of η and g when dividing it by $(\eta g)^2$. The following results therefore apply for any values of these two parameters, as long as they fulfill the condition which we specified in Eq. (17).

1. Dependence on the laser Rabi frequency

Fig. 3 shows the stationary state phonon number $m_{\rm ss}^{(0)}$ and the cooling rate $\gamma_{\rm c}^{(2)}$ as a function of the laser Rabi
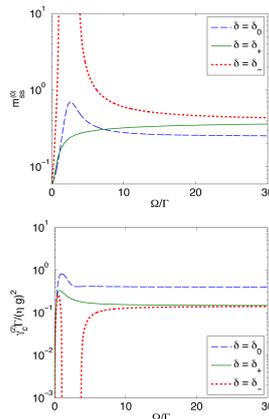
FIG. 3: (color online) Logarithmic plot of the stationary state phonon number $m_{\rm ss}^{(0)}$ and the cooling rate $\gamma_{\rm c}^{(2)}$ as a function of the laser Rabi frequency Ω, while $\nu = \kappa = \Gamma$.

frequency Ω. As suggested by Eq. (39), we find that there is no effective cooling, when the laser Rabi frequency Ω becomes very small. In the limit $\Omega \to 0$, the cooling rate $\gamma_{\rm c}^{(2)}$ tends for all three cooling resonances to zero. Although the stationary state phonon number $m_{\rm ss}^{(0)}$ might be relatively small, this case is of no interest, since the stationary state is reached only after a very long time. When Ω increases, also the cooling rate $\gamma_{\rm c}^{(2)}$ increases rapidly. Naively one might expect that increasing the laser Rabi frequency Ω further and further also increases the cooling rate further. This is not the case. As shown in Fig. 3, the cooling process saturates relatively quickly and the stationary state phonon number remains more or less constant for very large Ω.

When comparing all three cooling resonances, we see that the atom-cavity detuning δ_- yields the highest values of $m_{\rm ss}^{(0)}$ and is therefore of no practical interest. One reason for this can be found in Eqs. (1) and (14). For $\delta = \delta_-$, there is always a heating resonance relatively close by, which compensates some of the effects of the resonant cooling transition. Another reason for the relatively high values of $m_{\rm ss}^{(0)}$ for $\delta = \delta_-$ is that the ap-
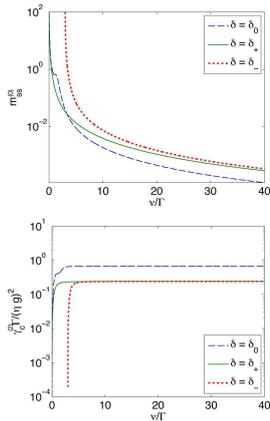
FIG. 4: (color online) Logarithmic plot of the stationary state phonon number $m_{\mathrm{ss}}^{(0)}$ and the cooling rate $\gamma_{\mathrm{c}}^{(2)}$ as a function of the phonon frequency ν for $\Omega = 3\,\Gamma$ and $\kappa = \Gamma$.

FIG. 5: (color online) Logarithmic plot of the stationary state phonon number $m_{\mathrm{ss}}^{(0)}$ and the cooling rate $\gamma_{\mathrm{c}}^{(2)}$ as a function of the phonon frequency ν for $\Omega = 30\,\Gamma$ and $\kappa = \Gamma$.

plied laser field creates a relatively large population in the state $|\lambda_+\rangle$ of the trapped particle, while the state $|\lambda_-\rangle$ remains less populated (cf. Eq. (29)). As one can see from Eq. (13), for $\delta = \delta_-$, the resonant annihilation of a phonon and the creation of a cavity photon is accompanied by an atomic transition from the state $|\lambda_-\rangle$ into $|\lambda_+\rangle$. When the average population in the state $|\lambda_-\rangle$ is relatively low, the atom is not well prepared to assist the cooling process when $\delta = \delta_-$.

In contrast to this, the system is in general well detuned from all heating transitions, when the atom-cavity detuning equals either δ_0 or δ_+. Moreover, for $\delta = \delta_+$ and for $\delta = \delta_0$, resonant cooling transitions are accompanied by a $|\lambda_+\rangle \rightarrow |\lambda_-\rangle$ and by a $|0\rangle \rightarrow |1\rangle$ or a $|1\rangle \rightarrow |0\rangle$ transition, respectively. Since the average population in the state $|\lambda_+\rangle$ and in the atomic states $|0\rangle$ and $|1\rangle$, respectively, is relatively large (see again Eq. (29)), the laser driving prepares the trapped particle well to facilitate the annihilation of a phonon and to assist the cooling process when $\delta = \delta_+$ or $\delta = \delta_0$. Indeed, Fig. 3 shows that the atom-cavity detuning δ_+ yields the lowest stationary state photon number $m_{\mathrm{ss}}^{(0)}$ for a relatively wide range of laser Rabi frequencies Ω. For the concrete parameters in
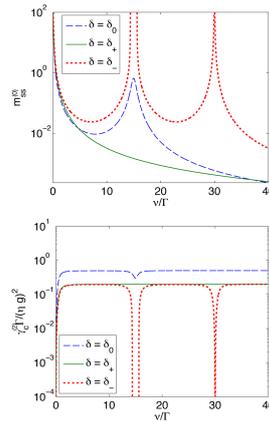
Fig. 3, this applies when Ω lies roughly between 2 and $7\,\Gamma$. For larger values of Ω, we obtain the lowest stationary state phonon number when choosing $\delta = \delta_0$ (sideband cooling case).

2. Dependence on the phonon frequency

Let us now have a closer look at the dependence of the cooling process on the phonon frequency ν. To do so, we consider a relatively small and a relatively large value of Ω, while keeping all other system parameters comparable to previous experimental parameters. As suggested by Fig. 3, we choose $\Omega = 3\,\Gamma$ (cf. Fig. 4) and $\Omega = 30\,\Gamma$ (cf. Fig. 5). In Fig. 5, we can easily identify two phonon frequencies ν for which certain cooling resonances (eg. δ_-) becomes identical to one of the heating resonances in Eq. (14). When this applies, the cooling rate $\gamma_{\mathrm{c}}^{(2)}$ becomes very small (in some cases it even becomes negative which implies heating) and $m_{\mathrm{ss}}^{(0)}$ tends to infinity. Moreover, in both figures, the atom-cavity detuning δ_- yields the highest stationary state phonon numbers and is therefore of less practical interest than δ_0
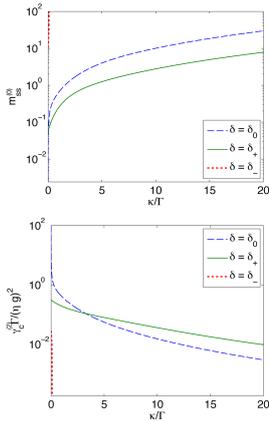
FIG. 6: (color online) Logarithmic plot of the stationary state phonon number $m_{\mathrm{ss}}^{(0)}$ and the cooling rate $\gamma_{\mathrm{c}}^{(2)}$ as a function of the spontaneous cavity decay rate κ for $\Omega = 3\,\Gamma$ and $\nu = \Gamma$.

FIG. 7: (color online) Logarithmic plot of the stationary state phonon number $m_{\mathrm{ss}}^{(0)}$ and the cooling rate $\gamma_{\mathrm{c}}^{(2)}$ as a function of the spontaneous cavity decay rate κ for $\Omega = 30\,\Gamma$ and $\nu = \Gamma$.

and δ_+. For relatively small phonon frequencies ν, the lowest stationary state phonon number is achieved, when the atom-cavity detuning equals δ_+. For very strongly confined particles, it is better to choose $\delta = \delta_0$ (sideband cooling case). As one would expect, we notice that higher phonon frequencies allow to cool the trapped particle to significantly lower temperatures.

3. Dependence on the spontaneous cavity decay rate

Finally, we discuss the dependence of $m_{\mathrm{ss}}^{(0)}$ and $\gamma_{\mathrm{c}}^{(2)}$ on the spontaneous cavity decay rate κ. As in the previous subsection, we choose $\Omega = 3\,\Gamma$ (cf. Fig. 6) and $\Omega = 30\,\Gamma$ (cf. Fig. 7). For a relatively wide range of experimental parameters, we find that the detuning δ_+ yields the lowest stationary state phonon number (cf. Figs. 6 and 7). This is especially then the case, when the spontaneous cavity decay rate κ is relatively large. Although this is not illustrated here, we would like to add that the cooling transitions become over-damped when κ becomes too large. In this case, the cooling becomes very inefficient and the stationary state phonon number $m_{\mathrm{ss}}^{(0)}$ increases
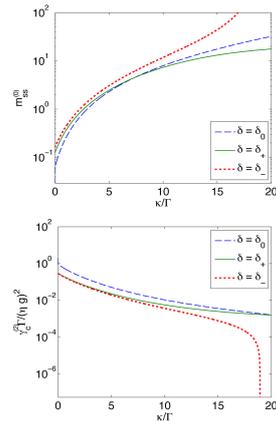
rapidly.

V. CONCLUSIONS

In this paper, we analyse cavity-mediated laser cooling for an atomic particle with external confinement in the direction of the cavity axis (cf. Fig. 1). The Hamiltonian H_{I} of this system contains an atom-phonon-photon interaction term which gives rise to three sharp resonances with a minimum stationary state phonon number. For a wide range of experimental parameters, for example, when the spontaneous cavity decay rate κ is relatively large or when the phonon frequency ν is relatively small, one should choose the atom-cavity detuning δ equal to δ_+ in Eq. (1) in order to minimise the stationary state phonon number m_{ss} (cf. Figs. 3–7). This resonance depends on the laser Rabi frequency Ω and is different from the usually considered resonance δ_0 for laser-sideband cooling.

To obtain an effective cooling rate γ_{c} and an analytical expression for the stationary state phonon number m_{ss} for the experimental setup which we consider in this

paper (cf. Eq. (39)), we proceed as in Refs. [25, 26, 28]. Starting from the standard quantum optical master equation, we derive linear differential equations – so-called rate or cooling equations – for the time evolution of expectation values. When taking a large enough number of expectation values into account, we obtain a closed set of equations, which can be used to analyse the time evolution of the mean phonon number m on a time scale given by η^2. The only assumption made in our calculations is that the atom-cavity coupling constant g multiplied with the Lamb-Dicke η is much smaller than at least one other experimental parameters (cf. Eq. (17)). The condition in Eq. (17) guarantees that the mean phonon number m evolves on a much slower time scale than all the other relevant expectation values and allows us to obtain Eq. (39) via an adiabatic elimination.

Achieving very low stationary state phonon numbers for a single trapped particle requires a relatively large phonon frequency ν, while very large spontaneous decay rates κ and Γ need to be avoided. Achieving relatively large cooling rates moreover requires a relatively large atom-cavity coupling constant g, since γ_c is proportional to $(\eta g)^2/\Gamma$. To overcome this problem, it might be interesting to study the cooling process of the experimental setup in Fig. 1 when it contains many trapped particles [33]. Using the same arguments as in Section III and diagonalising the system Hamiltonian with respect to its free energy and laser terms, one can show that many non-interacting particles experience exactly the same Mollow triplet of heating and cooling resonances as a single trapped particle.

[1] D. Wineland and H. Dehmelt, Bull. Am. Phys. Soc. **20**, 637 (1975).
[2] D. Leibfried, R. Blatt, C. Monroe, and D. Wineland, Rev. Mod. Phys. **75**, 281 (2003).
[3] B. L. Lev, A. Vukics, E. R. Hudson, B. C. Sawyer, P. Domokos, H. Ritsch, and J. Ye, Phys. Rev. A **77** 023402 (2008).
[4] K. Vigneron, *Etude d'effets de bistabilite optique induits par des atomes froids places dans une cavite optique*, Masters thesis Ecole Superieure d' Optique, (1995).
[5] P. Maunz, T. Puppe, I. Schuster, N. Syassen, P. W. H. Pinkse, and G. Rempe, Nature **428**, 50 (2004).
[6] S. Nussmann, K. Murr, M. Hijlkema, B. Weber, A. Kuhn, and G. Rempe, Nature Phys. **1**, 122 (2005).
[7] H. W. Chan, A. T. Black, and V. Vuletić, Phys. Rev. Lett. **90**, 063003 (2003).
[8] M. H. Schleier-Smith, I. D. Leroux, H. Zhang, M. A. Van Camp, and V. Vuletic, Phys. Rev. Lett. **107**, 143005 (2011).
[9] J. McKeever, J. R. Buck, A. D. Boozer, A. Kuzmich, H. C. Nägerl, D. M. Stamper-Kurn, and H. J. Kimble, Phys. Rev. Lett. **90**, 133602 (2003).
[10] M. J. Gibbons, S. Y. Kim, K. M. Fortier, P. Ahmadi, and M. S. Chapman, Phys. Rev. A **78**, 043418 (2008).
[11] T. Kampschulte, W. Alt, S. Brakhane, M. Eckstein, R. Reimann, A. Widera, and D. Meschede, Phys. Rev. Lett. **105**, 153603 (2010).
[12] M. Wolke, J. Klinner, H. Kessler, and A. Hemmerich, Science **337**, 75 (2012).
[13] B. L. Chuah, N. C. Lewty, R. Cazan, and M. D. Barrett, Phys. Rev. A **87**, 043420 (2013).
[14] T. W. Mossberg, M. Lewenstein, and D. J. Gauthier, Phys. Rev. Lett. **67**, 1723 (1991).
[15] T. Zaugg, M. Wilkens, P. Meystre, and G. Lenz, Opt. Comm. **97**, 189 (1993).
[16] P. Domokos and H. Ritsch, J. Opt. Soc. Am. B **20**, 1098 (2003).
[17] H. Ritsch, P. Domokos, F. Brennecke, and T. Esslinger, *Cold atoms in cavity-generated dynamical optical potentials*, arXive:1210.0013v2 (2013).
[18] V. Vuletić and S. Chu, Phys. Rev. Lett. **84**, 3787 (2000).
[19] K. Murr, Phys. Rev. Lett. **96**, 253001 (2006).
[20] M. Hemmerling and G. Robb, J. Mod. Opt. **58**, 1336 (2011).
[21] J. I. Cirac, A. S. Parkins, R. Blatt, and P. Zoller, Opt. Comm. **97**, 353 (1993).
[22] J. I. Cirac, M. Lewenstein, and P. Zoller, Phys. Rev. A **51**, 1650 (1995).
[23] A. Beige, P. L. Knight, and G. Vitiello, New J. Phys. **7**, 96 (2005).
[24] S. Zippilli and G. Morigi, Phys. Rev. Lett. **95**, 143001 (2005).
[25] T. Blake, A. Kurcz, and A. Beige, J. Mod. Opt. **58**, 1317 (2011).
[26] T. Blake, A. Kurcz, and A. Beige, Phys. Rev. A **86**, 013419 (2012).
[27] M. Bienert and G. Morigi, Phys. Rev. A **86**, 053402 (2012).
[28] T. Blake, A. Kurcz, N. S. Saleem, and A. Beige, Phys. Rev. A **84**, 053416 (2011).
[29] B. R. Mollow, Phys. Rev. **188**, 1969 (1969).
[30] E. del Valle and F. P. Laussy, Phys. Rev. Lett. **105**, 233601 (2010).
[31] A. Wickenbrock, P. Phoonthong, and F. Renzoni, J. Mod. Opt. **58**, 1310 (2011).
[32] It can be removed from the Hamiltonian, for example, by adding a minus sign to the excited electronic state $|1\rangle$.
[33] O. Kim *et al.* (in preparation).